Cellular/Molecular

Activity and Cytosolic Na^+ Regulate Synaptic Vesicle Endocytosis

Yun Zhu,[1*] Dainan Li,[1*] and Hai Huang[1,2]

[1]Department of Cell and Molecular Biology, Tulane University, New Orleans, Louisiana 70118, and [2]Tulane Brain Institute, Tulane University, New Orleans, Louisiana 70118

Retrieval of synaptic vesicles via endocytosis is essential for maintaining sustained synaptic transmission, especially for neurons that fire action potentials at high frequencies. However, how neuronal activity regulates synaptic vesicle recycling is largely unknown. Here we report that Na^+ substantially accumulated in the mouse calyx of Held terminals of either sex during repetitive high-frequency spiking. Elevated presynaptic Na^+ accelerated both slow and rapid forms of endocytosis and facilitated endocytosis overshoot, but did not affect the readily releasable pool size, Ca^{2+} influx, or exocytosis. To examine whether this facilitation of endocytosis is related to the Na^+-dependent vesicular content change, we dialyzed glutamate into the presynaptic cytosol or blocked the vesicular glutamate uptake with bafilomycin and found that the rate of endocytosis was not affected by regulating the vesicular glutamate content. Endocytosis is critically dependent on intracellular Ca^{2+}, and the activity of Na^+/Ca^{2+} exchanger (NCX) may be altered when the Na^+ gradient is changed. However, neither NCX inhibitor nor change of extracellular Na^+ concentration affected the endocytosis rate. Moreover, two-photon Ca^{2+} imaging showed that presynaptic Na^+ did not affect the action potential-evoked intracellular Ca^{2+} transient and decay. Therefore, we revealed a novel mechanism of cytosolic Na^+ in accelerating vesicle endocytosis. During high-frequency synaptic transmission, when large numbers of synaptic vesicles were fused, the rapid buildup of presynaptic cytosolic Na^+ promoted vesicle recycling and sustained synaptic transmission.

Key words: **axon terminal; calyx of Held; endocytosis; exoendocytic coupling; Na^+; spike**

Significance Statement

High-frequency firing neurons are widely distributed in the CNS. A large number of synaptic vesicles are released during high-frequency synaptic transmission; accordingly, synaptic vesicles need to be recycled rapidly to replenish the vesicle pool. Synaptic vesicle exocytosis and endocytosis are tightly coupled, and their coupling is essential for synaptic function and structural stability. We showed here that intracellular Na^+ concentration at the calyx of Held terminal increased rapidly during spike activity and the increased Na^+ accelerated endocytosis. Thus, when large numbers of synaptic vesicles are released during high-frequency synaptic transmission, Na^+ accumulated in terminals and facilitated vesicle recycling. These findings represent a novel cellular mechanism that supports reliable synaptic transmission at high frequency in the CNS.

Introduction

At chemical synapses, the fusion of synaptic vesicles with the presynaptic plasma membrane releases vesicular neurotransmitter contents for exerting various functions. Following exocytosis, membrane lipid bilayer and proteins are retrieved through endocytosis to form new vesicles (Sudhof, 2004; Kononenko and Haucke, 2015; Soykan et al., 2017). Different modes of endocytosis have been described in central synapses, including the classical clathrin-dependent endocytosis, kiss-and-run, and bulk endocytosis (Hosoi et al., 2009; Wu et al., 2009; Yamashita et al., 2010). Endocytosis in different conditions differs substantially in speed and amount. Slow endocytosis is mediated by a classical, clathrin- and dynamin-dependent endocytosis with a decay time constant (τ) of ~10 to 30 s, serving as the predominant mode for synaptic vesicle recycling during low-intensity activity (Granseth et al., 2006). The clathrin-independent, dynamin-dependent rapid endocytosis, with a τ within a few seconds, has been assumed to reflect kiss-and-run that involves rapid fusion pore opening and closure of the same vesicles after stronger stimulation (Alés et al., 1999; Wu et al., 2005). Bulk endocytosis occurs when large endosome-like structures are internalized from presynaptic plasma membrane during high-intensity firing

Received Jan. 15, 2020; revised June 18, 2020; accepted June 24, 2020.

Author contributions: Y.Z., D.L., and H.H. designed research; Y.Z., D.L., and H.H. performed research; Y.Z., D.L., and H.H. analyzed data; Y.Z., D.L., and H.H. wrote the paper.

*Y.Z. and D.L. contributed equally to this work.

Financial support was provided by US National Institutes of Health Grant R01-DC-016324 to H.H. We thank Dr. Laura Schrader, Youad Darwish, and Chen Wei Goh for critical reading of the manuscript.

The authors declare no competing financial interests.

Correspondence should be addressed to Hai Huang at hhuang5@tulane.edu.

https://doi.org/10.1523/JNEUROSCI.0119-20.2020

activity (Holt et al., 2003; Wu and Wu, 2007). Moreover, during intense stimulation and a massive influx of Ca^{2+}, the synaptic terminals may retrieve more membranes than vesicles being exocytosed. This phenomenon is defined as endocytosis overshoot that has been implicated in increasing endocytosis capacity and efficiency during high-frequency firing (Renden and von Gersdorff, 2007; Wu et al., 2009; Xue et al., 2012).

Accumulating evidence indicated that synaptic vesicle exocytosis and endocytosis are tightly coupled both temporally and spatially, and their timely coupling is essential for synaptic function and structural stability, but the underlying mechanism of this coupling is under debate. Ca^{2+} represents one prevalent possibility. Vesicle exocytosis is directly triggered by Ca^{2+}, while how Ca^{2+} regulates endocytosis is intricate and varies greatly in response to distinct neuronal activity (Leitz and Kavalali, 2016), making it complicated to coordinate endocytosis speed in an activity-dependent manner. Here we showed that action potential firing substantially elevated presynaptic cytosolic Na^+ in an activity-dependent manner in the mouse calyx of Held, a giant glutamatergic terminal in the auditory brainstem that fires continuous action potentials at high frequency up to hundreds of hertz. We found that the cytosolic Na^+ accelerated both slow and rapid forms of endocytosis and facilitated endocytosis overshoot, while the Na^+ effect on endocytosis was not implemented either through affecting Ca^{2+} influx or intracellular Ca^{2+} transients, or through regulating vesicular glutamate contents. Therefore, when large numbers of synaptic vesicles were fused during high-frequency synaptic transmission, Na^+ accumulated into presynaptic cytosol and facilitated vesicle recycling. Since the cytosolic Na^+ concentration is correlated with spike intensity and duration, it may work as a signal to coordinate vesicle endocytosis and recycling according to the level of exocytosis.

Materials and Methods

Slice preparation. The care and handling of animals were approved by the Institutional Animal Care and Use Committee of Tulane University and complied with US Public Health Service guidelines. Coronal brainstem slices containing the medial nucleus of the trapezoid body were prepared from postnatal day 8–12 C57BL/6J mice of either sex similar to those previously described (Zhang and Huang, 2017). Briefly, 210 μm slices were cut using a Vibratome (VT1200S, Leica) in ice-cold, low-Ca^{2+}, low-Na^+ saline containing the following (in mM): 230 sucrose, 10–25 glucose, 2.5 KCl, 0.1 $CaCl_2$, 3 $MgCl_2$, 1.25 NaH_2PO_4, 25 $NaHCO_3$, 0.4 ascorbic acid, 3 *myo*-inositol, and 2 Na-pyruvate, bubbled with 95% O_2/5% CO_2. Slices were incubated at 32°C for 20–30 min and thereafter stored at room temperature in normal artificial CSF (aCSF) contained the following (in mM): 125 NaCl, 10–25 glucose, 2.5 KCl, 1.2 $CaCl_2$, 1.8 $MgCl_2$, 1.25 NaH_2PO_4, 25 $NaHCO_3$, 0.4 ascorbic acid, 3 myo-inositol, and 2 Na-pyruvate, pH 7.4, bubbled with 5% CO_2/95% O_2 before use.

Membrane capacitance measurements. Slices were transferred to a recording chamber and perfused with bubbled aCSF (2–3 ml/min) warmed to ~32°C by an inline heater (Warner Instruments). Whole-cell recordings were made from calyces of Held with an EPC-10 USB patch-clamp amplifier with lock-in system and PatchMaster software (HEKA). For whole-cell membrane capacitance (C_m) measurements, the sinusoidal stimulus frequency was 1 kHz and the peak-to-peak voltage was 60 mV (Lindau and Neher, 1988). To isolate presynaptic Ca^{2+} currents in voltage-clamp experiments, TEA-Cl (10 mM), 4-aminopyridine (0.5 mM), and tetrodotoxin (1 μM) were added to aCSF, substituting for NaCl with equal osmolarity. For recordings of the endocytosis overshoot, $MgCl_2$ and $CaCl_2$ were adjusted to 1.0 and 2.0 mM, respectively, to facilitate overshoot (Wu et al., 2009; Xue et al., 2012). To test endocytosis under lowered extracellular Na^+ concentration, 50 mM NaCl was replaced by LiCl with equal osmolarity (Kim et al., 2005). The pipette solution contained the following (in mM): 70 Cs-methanesulfonate, 20 CsCl, 10 HEPES, 0.5 EGTA, 4 Mg-ATP, 0.3 $Tris_3$-GTP, 10 $Tris_2$-phosphocreatine, 5 glutamate, as well as 40 NMDG-methanesulfonate (for Na^+-free solution), 10 Na-methanesulfonate + 30 NMDG-methanesulfonate (for 10 mM Na^+ solution), or 40 Na-methanesulfonate (for 40 mM Na^+ solution). For presynaptic glutamate dialysis experiments, glutamate was added to substitute methanesulfonate with equal osmolarity. All solutions were adjusted to pH 7.3 with CsOH (310–315 mOsm). Tips of patch pipettes (3–5 MΩ) were coated with dental wax to reduce stray capacitance. Series resistance (<20 MΩ) was compensated up to 60% (10 μs lag). Data were obtained 4–20 min after break-in at sampling rate of 100 kHz and filtered with an online Bessel filter at 2.9 kHz.

Two-photon Na^+ and Ca^{2+} imaging. A Galvo multiphoton microscopy system (Scientifica) with a Ti:sapphire pulsed laser (Chameleon Ultra II, Coherent) was used for Na^+ and Ca^{2+} imaging. Whole-cell patch-clamp recordings were performed with a Multiclamp 700B amplifier and pClamp software (Molecular Devices). The laser was tuned to 800 nm for Na^+ imaging and 810 nm for Ca^{2+} imaging, and epifluorescence signals were captured through 60×, 1.0 numerical aperture (NA) objectives and a 1.4 NA oil-immersion condenser (Olympus). Fluorescence was split into red and green channels using dichroic mirrors and bandpass filters. Data were collected in frame-scan or line-scan modes using SciScan (Scientifica) or ScanImage (Vidrio Technologies). Presynaptic spikes were evoked by afferent fiber stimulation or current injection and recorded under current clamp, and corresponding Ca^{2+} and Na^+ signals were recorded under two-photon imaging.

For Ca^{2+} imaging under different Na^+ concentrations, the pipette solution contained the following (in mM): 70 K-methanesulfonate, 20 KCl, 10 HEPES, 4 Mg-ATP, 0.3 $Tris_3$-GTP, 10 $Tris_2$-phosphocreatine, 5 glutamate, as well as 40 NMDG-methanesulfonate (for Na^+-free solution), 10 Na-methanesulfonate + 30 NMDG-methanesulfonate (for 10 mM Na^+ solution), or 40 Na-methanesulfonate (for 40 mM Na^+ solution). For Ca^{2+} imaging with bath application of KB-R7943, the pipette solution contained the following (in mM): 130 K-gluconate, 20 KCl, 4 MgATP, 0.3 Tris-GTP, 7 Na_2-phosphocreatine, and 10 HEPES. All solutions were adjusted to 290 mOsm, pH 7.3 with KOH; 250 μM Fluo-5F and 20 μM Alexa Fluor 594 were also added to the pipette solutions before the experiments. Data are expressed as $\Delta(G/R)/(G/R)_{max} \times 100\%$, where $(G/R)_{max}$ is the maximal fluorescence in saturating Ca^{2+} (Spratt et al., 2019).

For Na^+ imaging, pipette solution contained the following (in mM): 110 K-methanesulfonate, 20 KCl, 10 HEPES, 0.5 EGTA, 4 Mg-ATP, 0.3 $Tris_3$-GTP, and 5 Na_2-phosphocreatine, 290 mOsm and pH 7.3 with KOH, while 1 mM sodium-binding benzofurane isophthalate (SBFI) and 15 μM Alexa Fluor 594 were added before the experiments. To avoid the perfusion of cytoplasmic Na^+ during resting and spike-evoked Na^+ signals recordings, pipettes were subsequently detached after whole-cell dialysis with SBFI and Alexa Fluor 594 dyes when the fluorescence intensities were stable and Na^+ signals were measured after waiting at least 10 min. Standard calibration methods were used to measure absolute Na^+ concentrations (Rose, 2012; Huang and Trussell, 2014). After loading fluorescent dyes through whole-cell recordings, pipettes were detached for resting [Na^+] and calibration. The solutions for *in situ* calibration of SBFI fluorescence contained the following (in mM): 20 KCl, 25 glucose, 10 HEPES, and 130 (K-gluconate + Na-gluconate), and adjusted to pH 7.4 with KOH; 3 μM gramicidin D, 10 μM monensin, and 50 μM ouabain were added into the calibration solutions before experiments.

Drugs. Drugs were obtained from Alomone Labs (tetrodotoxin), LC Laboratories (bafilomycin A1), and Thermo Fisher Scientific (SBFI, fluo-5F, and Alexa Fluor 594), and all others were obtained from Sigma-Aldrich. Bafilomycin A1 and KB-R7943 were prepared with DMSO, stored at −20°C, and dissolved in aCSF immediately before experiments.

Analysis. Data were analyzed using PatchMaster (HEKA), Clampfit (Molecular Devices), Igor (WaveMetrics), and ImageJ (NIH). Liquid junction potentials (10–11 mV) were measured and adjusted appropriately. The following standard monoexponential functions were used to describe slow endocytosis: $f(t) = A \times e^{-t/\tau} + C$, where A is the capacitance jump (ΔC_m) and τ is the time constant. Double exponential functions were used to describe endocytosis under strong stimulations, as

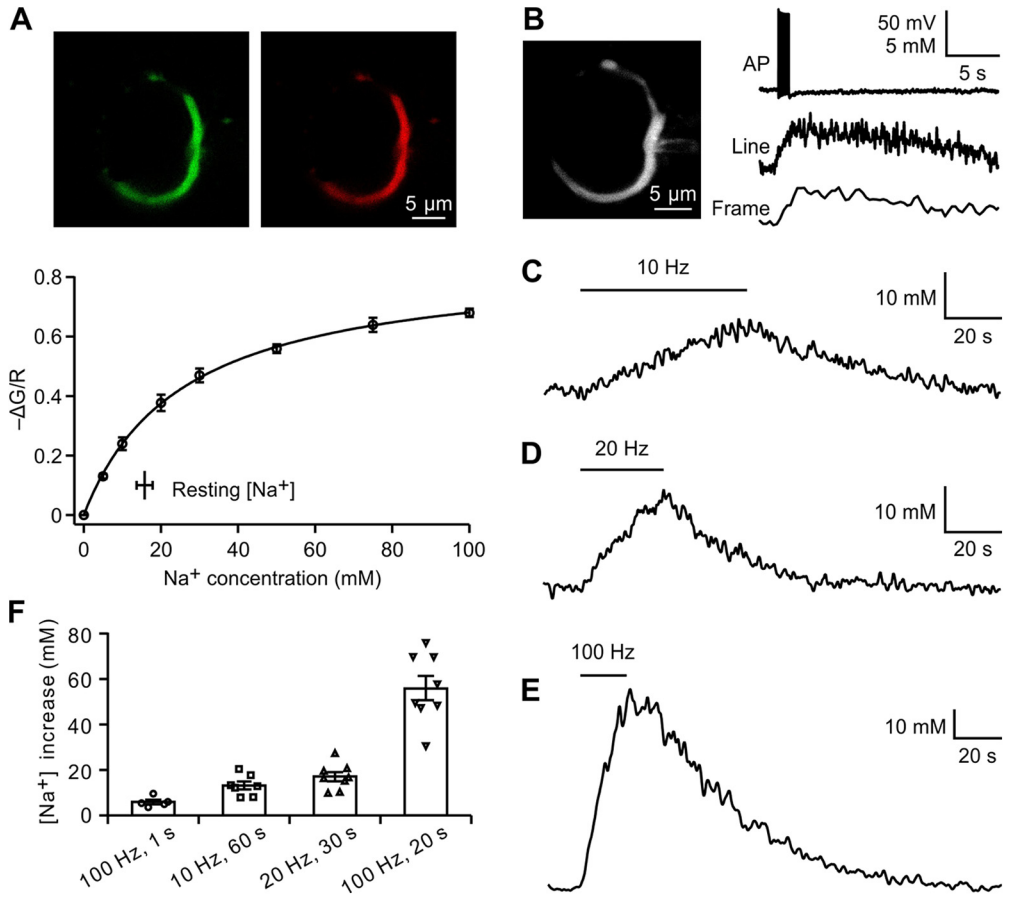

Figure 1. Presynaptic spikes control cytosolic Na^+ concentration. ***A***, *In situ* calibration of SBFI fluorescence under two-photon microscopy. Top, Single optical section of a calyx of Held terminal filled with SBFI (green) and Alexa Fluor 594 (red) through whole-cell recording. The recording pipette was subsequently detached for resting $[Na^+]$ measurement and $[Na^+]$ calibration. Bottom, Change in fluorescence with $[Na^+]_i$ ($n = 5$). The fitted curve yielded a K_{app} of 25.7 mM and $(G/R)_{max}$ of −0.86 for SBFI (see Materials and Methods). The resting $[Na^+]_i$ was shown in the insert. ***B***, A calyx of Held filled with SBFI and Alexa Fluor 594 under whole-cell recording. Spikes were evoked at 100 Hz for 1 s by afferent fiber stimulation. An increase in $[Na^+]$ was visualized under line-scan and frame-scan modes. ***C–E***, After detaching recording pipettes from calyces, Na^+ signals in response to increasing spike frequencies were measured. Spikes at 10 Hz (***C***), 20 Hz (***D***), and 100 Hz (***E***) induced different changes in intracellular Na^+ concentration. ***F***, Summary of results of presynaptic Na^+ increases under different stimulations. Error bars indicate ±SEM.

follows: $f(t) = A_1 \times e^{-t/\tau 1} + A_2 \times e^{-t/\tau 2} + C$, where A_1 and A_2 are the amplitudes of fast and slow exponential components; and τ_1 and τ_2 are the time constants of each component, respectively. The weighted time constant is expressed: $\tau_{weight} = (A_1 \times \tau_1 + A_2 \times \tau_2)/(A_1 + A_2)$. For Na^+ calibration, data are normalized and fitted by the following equation: $(\Delta G/R) = (G/R)_{max} \times [Na^+]_i/([Na^+]_i + K_{app})$, where G/R is the ratio of green fluorescence relative to red fluorescence; (ΔG/R) is the change in fluorescence ratio measured at a given $[Na^+]_i$ divided by that at 0 mM $[Na^+]_i$; $(G/R)_{max}$ is the maximal change in fluorescence ratio and K_{app} is the apparent K_d of SBFI. Data were presented as the mean ± SEM. Statistical significance was established using one-way ANOVA followed by Tukey's multiple-comparisons test, as well as paired and unpaired *t* tests as indicated, with $p < 0.05$ indicating a significant difference.

Results

Spikes activity increases presynaptic cytosolic Na^+ concentration

Changes in presynaptic Na^+ during action potential (AP) firing were assayed using Na^+ imaging with two-photon laser scanning microscopy. Calyces of Held were loaded via whole-cell recordings with the Na^+ indicator SBFI and the volume marker Alexa Fluor 594. Standard calibration methods (Rose, 2012; Huang and Trussell, 2014) were used to measure the absolute $[Na^+]$ (Fig. 1*A*). The presynaptic $[Na^+]$ at the resting state was 15.8 ± 2.1 mM ($n = 4$). APs were evoked by afferent fiber stimulation and propagated to the presynaptic terminals. Upon 100 Hz stimulation for 1 s, presynaptic cytosolic $[Na^+]$ increased by 5.7 ± 1.1 mM, which decayed to the control level with a time constant of 12.2 ± 1.0 s ($n = 5$; Fig. 1*B*). After ensuring reliable AP evocation by afferent fiber stimulation, the recording pipettes were subsequently detached from the calyces, and the Na^+ signals on stimulations at different frequencies were measured. Spiking at 10 Hz for 60 s reversibly increased the $[Na^+]$ by 12.2 ± 1.7 mM ($n = 7$; Fig. 1*C*). Na^+ transients were gradually augmented as increasing spike frequency, as follows: 20 Hz for 30 s increased the $[Na^+]$ by 16.3 ± 2.0 mM ($n = 8$; Fig. 1*D*) and 100 Hz for 20 s increased the $[Na^+]$ by 55.6 ± 5.9 mM ($n = 8$; Fig. 1*E*). Therefore, spike activities efficiently increase the presynaptic cytosolic Na^+ concentration in an activity-dependent manner (Fig. 1*F*).

Presynaptic cytosolic Na^+ facilitates slow endocytosis

Capacitance measurements were made at the calyx of Held terminals to examine whether presynaptic Na^+ influences vesicle endocytosis and recycling. Endocytosis of the calyces depends on the intensity of activity. Mild stimulations such as single pulses of 1–40 ms depolarization trigger slow clathrin-dependent endocytosis, while stronger stimulations such as 10 pulses of 20 ms depolarization induce an additional clathrin-independent rapid form of endocytosis (Wu et al., 2005, 2009; Hosoi et al., 2009; Yamashita et al., 2010). We measured the whole-cell capacitance

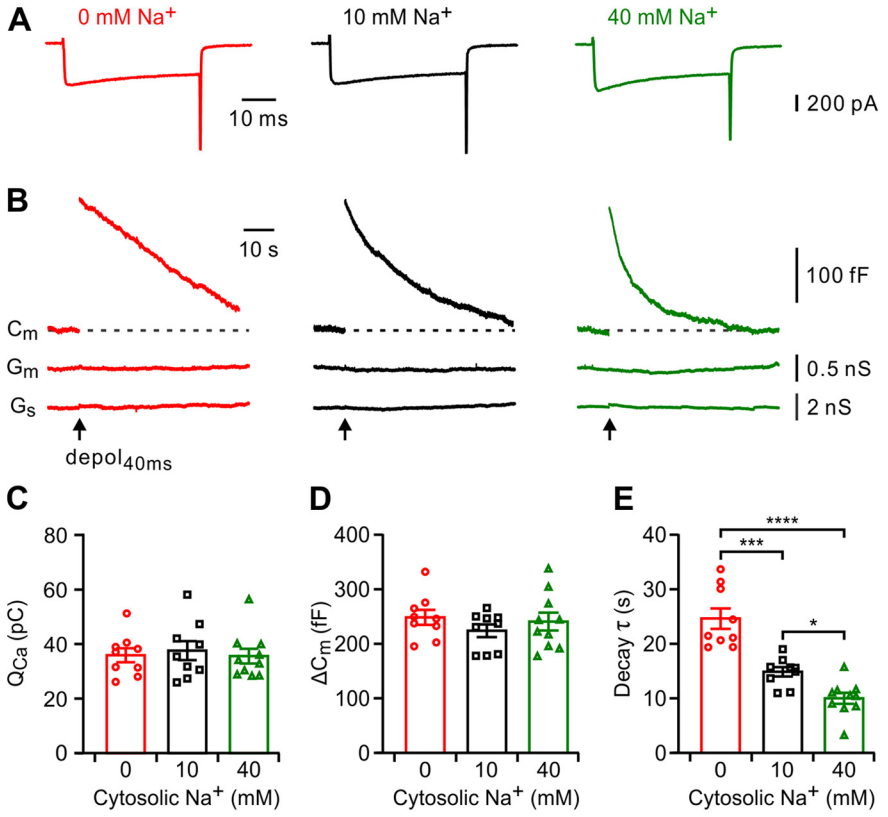

Figure 2. Presynaptic Na^+ facilitates slow endocytosis without affecting exocytosis. ***A***, Sampled presynaptic Ca^{2+} currents induced by 40 ms depolarizations from −80 to +10 mV ($depol_{40ms}$) with presynaptic pipette solutions containing 0 mM (left), 10 mM (middle), or 40 mM Na^+ (right). ***B***, Corresponding C_m recordings showing exocytosis and endocytosis induced by $depol_{40ms}$. Membrane conductance (G_m) and series conductance (G_s) are included to confirm the recording stability. ***C–E***, Group data of the effects of cytosolic Na^+ on Ca^{2+} charge (Q_{Ca}; ***C***), capacitance jump (ΔC_m; ***D***), and the time constant of capacitance decay (τ; ***E***). $^*p < 0.05$, $^{***}p < 0.001$, $^{****}p < 0.0001$; Tukey's multiple-comparisons test. Error bars indicate ±SEM.

under 1.2 mM extracellular Ca^{2+} at 32°C with pipette solutions containing 0, 10, or 40 mM Na^+. A voltage depolarization from −80 to +10 mV for 40 ms ($depol_{40ms}$) induced Ca^{2+} influx and triggered ΔC_m, followed by slow C_m decay toward to the prestimulus level (Fig. 2). Because C_m is proportional to the membrane surface area, ΔC_m reflects exocytosis and C_m decay reflects endocytosis (Sun and Wu, 2001). This protocol is sufficient to release the readily releasable vesicles (Wu and Borst, 1999; Fedchyshyn and Wang, 2005; Renden and von Gersdorff, 2007), with ΔC_m reflecting the size of readily releasable pool. We found that the Ca^{2+} currents ($p = 0.87$) and ΔC_m ($p = 0.47$; one-way ANOVA test) were not different in recordings with 0, 10, or 40 mM Na^+ (Fig. 2*C*,*D*), while presynaptic Na^+ showed profound effects on the endocytosis rate (Fig. 2*E*). When the terminal was dialyzed with 10 mM Na^+, the C_m decay could be fitted with a monoexponential function with a time constant (τ) of 15.3 ± 0.9 s ($n = 9$). With the 40 mM Na^+ solution dialyzed presynaptically, the endocytosis rate accelerated, and the time constant reduced to 10.4 ± 1.0 s ($n = 10$). Upon dialysis with Na^+-free solution, the endocytosis became slower, resulting in a time constant of 25.1 ± 1.9 s ($n = 9$; $p < 0.0001$, one-way ANOVA followed by Tukey's multiple-comparisons test). Thus, presynaptic cytosolic Na^+ accelerates slow endocytosis induced by single depolarizing steps.

Cytosolic Na^+ facilitates rapid endocytosis

Stronger stimulation induces a clathrin-independent rapid form of endocytosis along with the slow endocytosis (Alés et al., 1999; Wu et al., 2005), so we next investigated whether Na^+ modulates the rapid form of endocytosis. With 10 mM Na^+ in the presynaptic solution, 10 pulses of 20 ms depolarization from −80 to +10 mV at 10 Hz ($depol_{20ms} \times 10$) evoked a ΔC_m of 1002 ± 55 followed by a C_m decay that can be fitted with a double exponential function whose fast and slow time constants were 3.3 ± 0.3 and 15.1 ± 1. 9 s, respectively (Fig. 3). The fast component was 40.1 ± 2.7% of the fit (the remainder being slow component), and the weighted mean was 11.5 ± 1.1 s ($n = 11$). When the terminal was dialyzed with 40 mM Na^+, both fast and slow endocytosis were accelerated, resulting in fast and slow components of 1.3 ± 0.2 s (36.4 ± 3.4%) and 10. 8 ± 1.1 s, respectively, and a weighted time constant of 7.6 ± 0.8 s ($n = 11$), while Na^+-free solution slowed down both fast and slow endocytosis to 4.9 ± 0.6 s (36. 6 ± 4.7%) and 22.6 ± 2.1 s, respectively, and a weighted time constant of 18.3 ± 1.8 s ($n = 10$; $p < 0.0001$, one-way ANOVA). The evoked ΔC_m was not different among groups (Fig. 3*E*; $p = 0.67$, one-way ANOVA). These results revealed that presynaptic cytosolic Na^+ facilitates both the slow and rapid modes of synaptic vesicle endocytosis induced by repetitive depolarization steps.

Cytosolic Na^+ facilitates endocytosis overshoot

During intense stimulations, such as 10 depolarization pulses of 50 ms at 10 Hz ($depol_{50ms} \times 10$), the calyx terminal could retrieve more membranes than exocytosed, and induced endocytosis overshoot (Renden and von Gersdorff, 2007; Wu et al., 2009; Xue et al., 2012). We then tested whether Na^+ influences the endocytosis overshoot, in which an extracellular solution containing 2 mM Ca^{2+} was used to increase the chance of the observation (Wu et al., 2009; Xue et al., 2012). The size of endocytosis overshoot was quantified as the capacitance value below the baseline at 40~60 s after depolarization pulses (Wu et al., 2009). We found that increased Na^+ concentrations facilitated the observation of endocytosis overshoot. As the [Na^+] increased from 0 to 10, and 40 mM, the percentage of cells with overshoot increased from 28.6% (two of seven calyces) to 66.7% (six of nine calyces), and 100% (seven of seven calyces). For the cells that showed overshoot, the overshoot ratio increased from 5.5 ± 4.4% to 14.7 ± 3.0%, and 22.8 ± 4.3% (Fig. 4; $p = 0.0008$, one-way ANOVA). These results indicate that the cytosolic Na^+ also facilitates endocytosis overshoot in both the percentage of cells and the size of the membrane area.

Vesicular content does not affect slow or rapid endocytosis

A previous study showed that cytosolic transmitter concentration, which rapidly controls the vesicular neurotransmitter contents (Hori and Takahashi, 2012; Apostolides and Trussell, 2013), regulates vesicle cycling at hippocampal GABAergic terminals in culture (Wang et al., 2013). Since presynaptic Na^+ facilitates vesicular glutamate transport and higher cytosolic

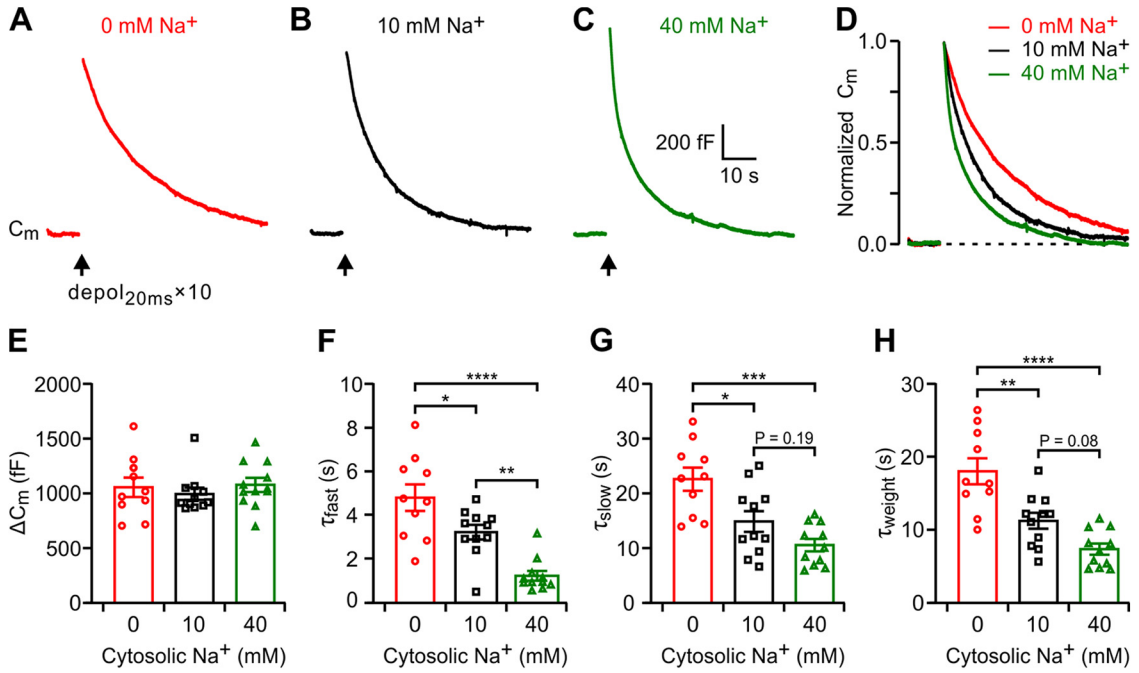

Figure 3. Cytosolic Na^+ facilitates rapid endocytosis. ***A–C***, Sampled C_m recordings showing exocytosis and endocytosis induced by 10 of 20 ms depolarizations ($depol_{20ms}$ × 10) with pipette solutions containing 0 mM (***A***), 10 mM (***B***), or 40 mM (***C***) Na^+. ***D***, Normalized C_m traces of ***A–C*** showing the Na^+ effects on endocytosis rate. ***E***, Statistics for ΔC_m. ***F–H***, The capacitance decay was fitted by double exponentials. The fast (τ_{fast}; ***F***) and slow (τ_{slow}; ***G***) components, and the weighted mean (τ_{weight}; ***H***) from different cytosolic Na^+ concentrations were compared. $^*p < 0.05$, $^{**}p < 0.01$, $^{***}p < 0.001$, $^{****}p < 0.0001$; Tukey's multiple-comparisons test. Error bars indicate ±SEM.

$[Na^+]$ increases the vesicle glutamate contents (Huang and Trussell, 2014; Li et al., 2020), we performed two lines of experiment to test whether the effects of Na^+ on endocytosis occur through regulating vesicular contents (Fig. 5). First, we performed capacitance measurements under different concentrations of cytosolic glutamate (0, 5, or 50 mM), which allows the manipulation of vesicular glutamate content (Hori and Takahashi, 2012), while keeping the cytosolic $[Na^+]$ constant at 10 mM. Slow and rapid endocytosis were evoked by the weak ($depol_{40ms}$; Fig. 5*A*) and intense ($depol_{20ms}$ × 10; Fig. 5*E*) stimulations, respectively. Our results showed that neither the slow ($p = 0.82$, one-way ANOVA; Fig. 5*D*) nor the rapid ($p = 0.74$, one-way ANOVA; Fig. 5*H*) mode of endocytosis was influenced by the cytosolic glutamate concentration. Second, we tested the effects of bafilomycin, a V-ATPase inhibitor that impedes vesicle acidification and neurotransmitter reloading, on endocytosis triggered by the same protocols (Fig. 5*B*,*F*). The results showed that 2 μM bafilomycin affected neither slow ($p = 0.30$, unpaired *t* test; Fig. 5*D*) nor rapid endocytosis ($p = 0.56$, unpaired *t* test; Fig. 5*H*). The exocytoses were not different among all groups (Fig. 5*C*,*G*). These results indicate that vesicular content had no significant effects on exocytosis or endocytosis.

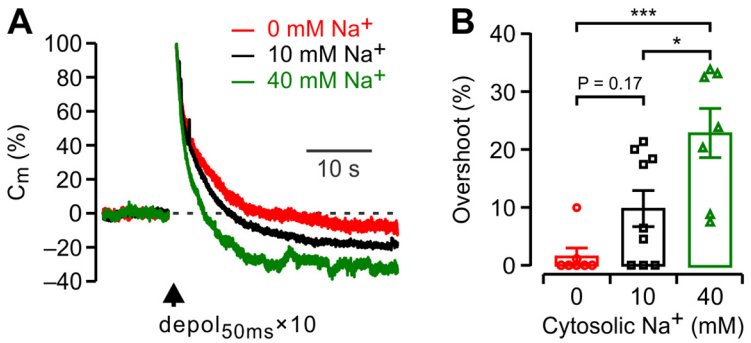

Figure 4. Cytosolic Na^+ facilitates endocytosis overshoot. ***A***, Sampled endocytosis overshoots induced by 10 50 ms depolarizations ($depol_{50ms}$ × 10) with presynaptic pipette solutions containing 0, 10, or 40 mM Na^+. Extracellular Ca^{2+} was elevated to 2 mM to increase the chance of observing overshoot. ***B***, Statistics for endocytosis overshoot size in the three groups. $^*p < 0.05$, $^{***}p < 0.001$; Tukey's multiple-comparisons test. Error bars indicate ±SEM.

Cytosolic Na^+ facilitated endocytosis is independent of NCX activity

It has been shown that plasma membrane Na^+/Ca^{2+} exchanger (NCX) is involved in maintaining presynaptic Ca^{2+} homeostasis (Kim et al., 2005), while Ca^{2+} plays specific roles in synaptic vesicle endocytosis (Leitz and Kavalali, 2016). To test whether presynaptic cytosolic Na^+ affects endocytosis by regulating NCX function, we lowered the extracellular Na^+ concentration to mimic the Na^+ concentration gradient change in elevated intracellular Na^+ conditions. As shown in Figure 6*A–C*, the endocytosis rate was not changed by lowering extracellular Na^+ for 50 mM ($p = 0.50$, $n = 6$, paired *t* test). We also tested whether inhibiting NCX activity directly affects the endocytosis rate. As shown in Figure 6*D–F*, incubation with the NCX inhibitor KB-R7943 (20 μM) slightly but not significantly slowed the rate of endocytosis ($n = 8$; $p = 0.14$, paired *t* test). To confirm that KB-R7943 indeed inhibited Na^+/Ca^{2+} exchange activity, we performed two-photon Ca^{2+} imaging with Fluo-5F. Ca^{2+} influx was evoked by 10 APs at 100 Hz. KB-R7943 did not affect the peak Ca^{2+} signal ($p = 0.26$, $n = 5$), while the decay time constant was increased from 0.57 ± 0.07 to 0.84 ± 0.13 s (Fig. 6*G–I*; $n = 5$; $p = 0.02$,

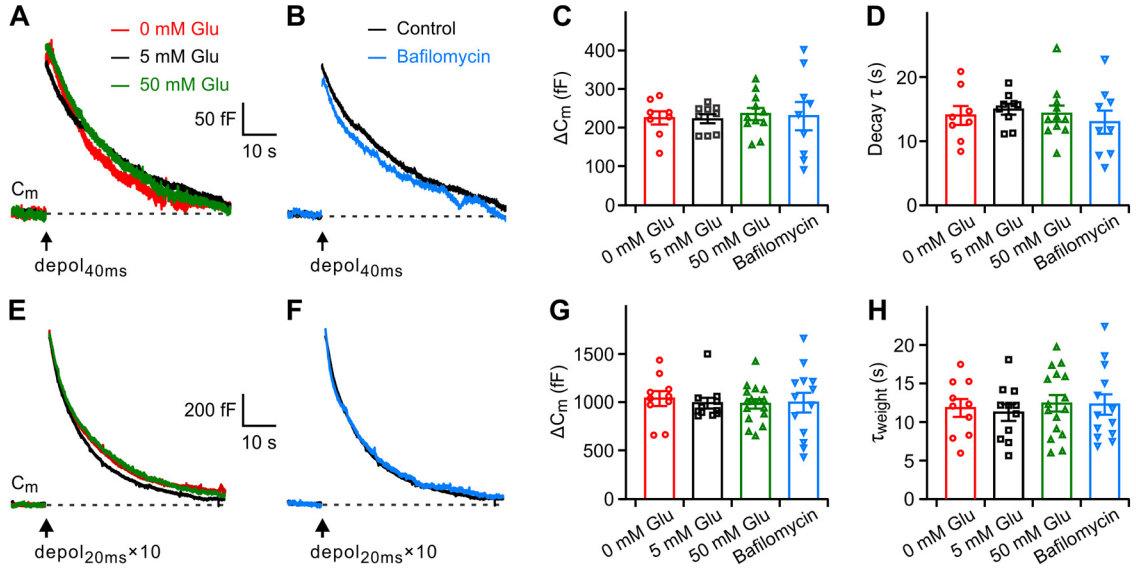

Figure 5. Vesicular glutamate content does not affect the endocytosis rate. ***A***, ***B***, Slow endocytosis induced by $depol_{40ms}$ when pipette solutions contained 0, 5, or 50 mM glutamate (***A***), or after incubating bafilomycin A1 (***B***). ***C***, ***D***, Neither glutamate nor bafilomycin affected the capacitance jump ΔC_m (***C***) or the time constant of capacitance decay τ (***D***). ***E–H***, Similar to ***A–D***, while rapid endocytosis was induced by $depol_{20ms} \times 10$. Error bars indicate ±SEM.

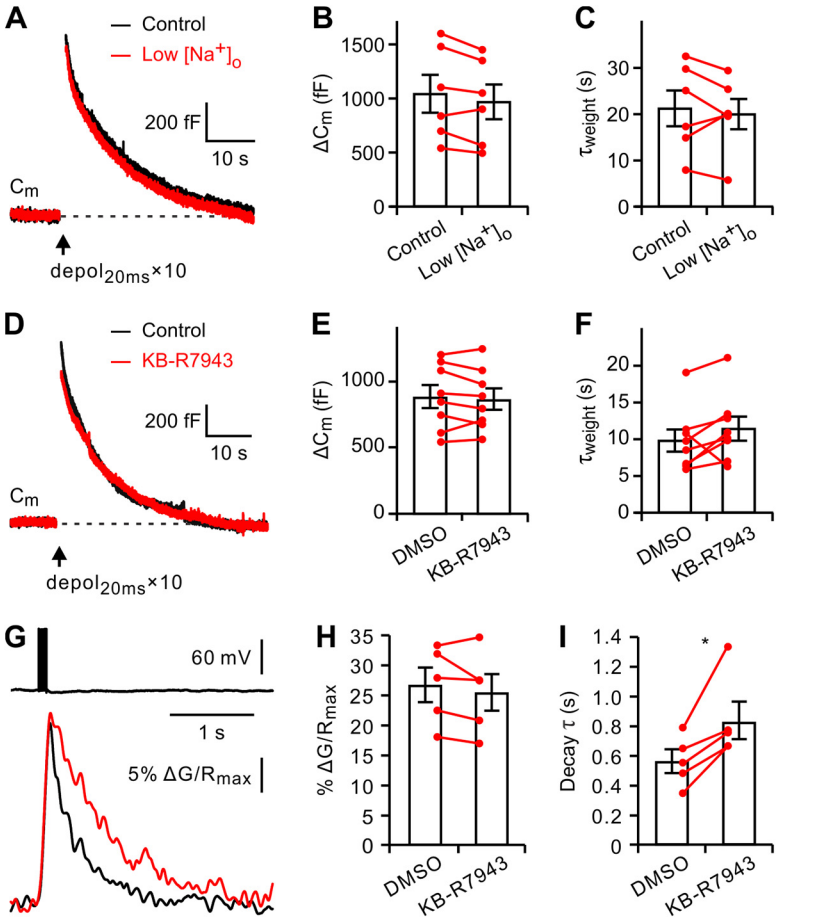

Figure 6. Facilitation of endocytosis by Na^+ does not occur through affecting Na^+/Ca^{2+} exchange activity. ***A***, ***D***, Sampled C_m recordings showing exocytosis and endocytosis induced by 10 20 ms depolarizations ($depol_{20ms} \times 10$) in control and with low extracellular Na^+ concentration (***A***) or in the presence of NCX inhibitor KB-R7943 (***D***). ***B***, ***C***, Low extracellular Na^+ did not affect the ΔC_m (***B***) or the weighted time constant of capacitance decay (τ_{weight}; ***C***). ***E***, ***F***, KB-R7943 did not affect ΔC_m (***E***) or τ_{weight} (***F***). ***G–I***, Two-photon Ca^{2+} imaging showing that the spike-evoked Ca^{2+} decay was slowed by KB-R7943 while the peak of Ca^{2+} transients stayed unchanged. *$p < 0.05$. Error bars indicate ±SEM.

paired *t* test). On the other hand, if Na^+ regulates endocytosis through slowing NCX-dependent Ca^{2+} extrusion, one would, however, expect an acceleration of endocytosis by NCX inhibitor. Therefore, the presynaptic Na^+-regulated vesicle recycling is not mediated by modulating NCX function or Ca^{2+} extrusion.

Cytosolic Na^+ does not affect spike-evoked intracellular Ca^{2+} rise and decay

To test whether cytosolic Na^+ affects intracellular Ca^{2+} dynamics during spiking activity, we made two-photon Ca^{2+} imaging with Fluo-5F loaded into the presynaptic terminal (Fig. 7). Calyces were recorded with pipette solutions containing 0, 10, or 40 mM Na^+. A burst of 10 APs at 100 Hz evoked a rapid Ca^{2+} rise of similar concentrations at all concentrations of Na^+ tested, as indicated by the fluorescence increases of 29.3 ± 0.9% of $(G/R)_{max}$ in Na^+-free ($n = 8$), 30.3 ± 1.5% in 10 mM Na^+ ($n = 7$), and 31.3 ± 1.6% in 40 mM Na^+ ($n = 6$) pipette solutions (Fig. 7*C*). The Ca^{2+} signals decayed to the background level within seconds and were not different among groups. The Ca^{2+} decay time constants were 0.56 ± 0.06 s for 0 mM Na^+, 0.60 ± 0.07 s for 10 mM Na^+, and 0.61 ± 0.05 s for 40 mM Na^+ solutions ($p = 0.80$, one-way ANOVA; Fig. 7*D*). Thus, it is unlikely that the cytosolic Na^+ facilitates endocytosis through a Ca^{2+}-dependent mechanism.

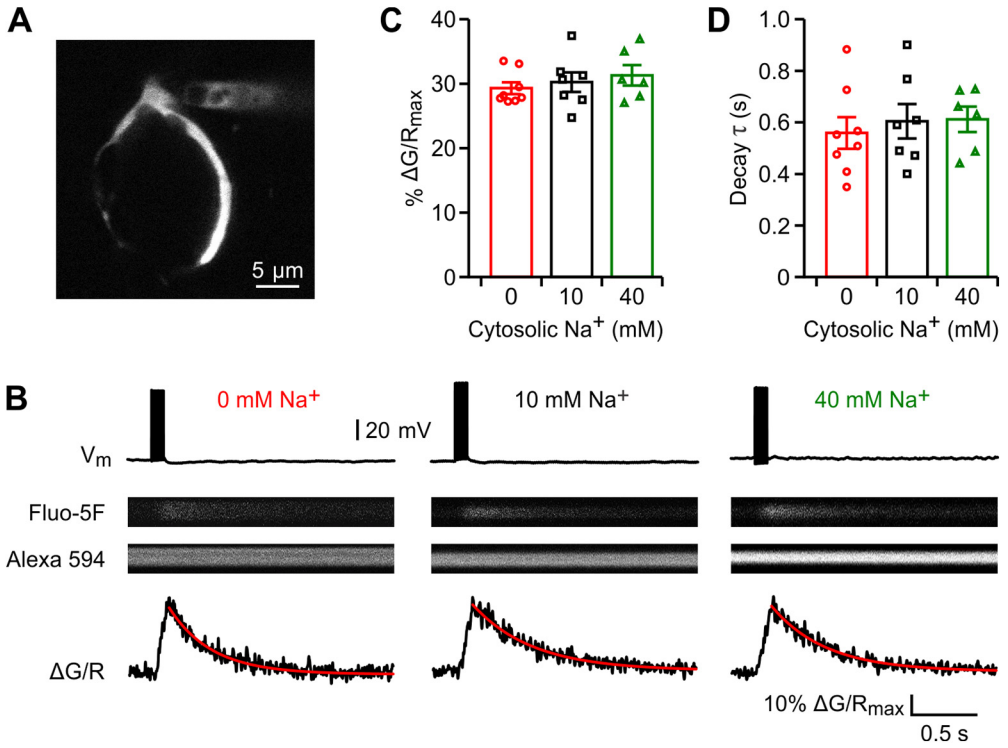

Figure 7. Cytosolic Na^+ does not affect spike-evoked Ca^{2+} transients and decay. ***A***, Single optic section of the calyx with attached patch pipette. ***B***, Presynaptic Ca^{2+} transients induced by 10 spikes at 100 Hz when dialyzed with a pipette solution containing 0, 10, or 40 mM Na^+. ***C***, ***D***, Summary plots of relative Ca^{2+} rise and decay times with different intracellular Na^+ concentrations. Error bars indicate ±SEM.

Discussion

Here we showed that intracellular Na^+ concentration at the presynaptic terminal increased rapidly during spike activity (Fig. 1). This elevated [Na^+] accelerated slow (Fig. 2) and rapid endocytosis (Fig. 3), and facilitated endocytosis overshoot (Fig. 4). The modulation of endocytosis by Na^+ was unlikely related to vesicular glutamate contents (Fig. 5), Ca^{2+} influx through NCX (Fig. 6), or intracellular Ca^{2+} transients in response to stimulation (Fig. 7). Therefore, we revealed an unappreciated role of cytosolic Na^+ in the regulation of synaptic vesicle endocytosis and recycling. When large numbers of synaptic vesicles are fused during high-frequency synaptic transmission, accumulated presynaptic Na^+ accelerates vesicle recycling and sustains synaptic transmission, representing a novel cellular mechanism that supports reliable synaptic transmission at high- frequency in the CNS.

Accumulating evidence indicated that synaptic vesicle exocytosis and endocytosis are tightly coupled both temporally and spatially, and their coupling is essential for synaptic function and structural stability. During prolonged high-frequency synaptic transmission, when large numbers of synaptic vesicles are fused with presynaptic membrane, endocytosis needs to be accelerated to replenish the vesicle pool and maintain the strength of synaptic transmission. Slow endocytosis and vesicle recycling lead to depletion of the release-ready vesicles, which have been shown to be a major contribution to short-term depression (von Gersdorff and Borst, 2002; Fernández-Alfonso and Ryan, 2004; Regehr, 2012). Different mechanisms have been observed to couple endocytosis with exocytosis, including Ca^{2+} (Sankaranarayanan and Ryan, 2001; Hosoi et al., 2009; Wu et al., 2009), membrane lipids such as PIP2 (Koch and Holt, 2012), and cytoskeleton proteins (Yuan et al., 2015; Orlando et al., 2019). Ca^{2+}-dependent regulation of exoendocytosis coupling has been prevalently studied. Exocytosis is directly triggered by Ca^{2+}, and endocytosis is regulated by Ca^{2+}-dependent mechanisms. (Wu et al., 2014). Ca^{2+} speeds up slow, rapid, and bulk endocytosis, while buffering intracellular Ca^{2+} with chelators or reducing Ca^{2+} influx slows down endocytosis in endocrine cells and various synapses (Sankaranarayanan and Ryan, 2001; Hosoi et al., 2009; Wu et al., 2009). However, increased Ca^{2+} influx during prolonged stimulation train slows down endocytosis in many preparations, including chromaffin cells, neuromuscular junction, retinal ribbon terminals, and central synapses (von Gersdorff and Matthews, 1994; Wu and Betz, 1996; Sun et al., 2002, 2010; Elhamdani et al., 2006; Balaji et al., 2008). A recent study showed that the dynamics of Ca^{2+} concentration changes can differentially modulate endocytosis. Specifically, transient large calcium increases trigger endocytosis, while prolonged small global Ca^{2+} increases inhibit slow endocytosis (Wu and Wu, 2014). Therefore, the regulation of endocytosis by Ca^{2+} concentration is complex and varies greatly in response to distinct neuronal activity, making it complicated to coordinate endocytosis speed in an activity-dependent manner.

Neural activity is provided by ion fluxes through voltage and neurotransmitter-gated channels, and spiking activity alters ion composition in the cytosol. Although the intracellular K^+ concentration is high and relatively stable, the Ca^{2+} and Na^+ levels are dynamically regulated during activity. We showed that the presynaptic cytosolic Na^+ of the mouse calyx of Held is 15.8 ± 2.1 mM, very similar to that of the rat calyx (Huang and Trussell, 2014). We previously reported that calyceal terminals express Na^+-permeable HCN channels, and the activation of HCN channels contributes to the resting Na^+ concentration of 4.9 ± 0.5 mM (Huang and Trussell, 2014). Here we found that spikes are much more potent in regulating presynaptic Na^+ accumulation than HCN channels. Upon 1 s of 100 Hz firing, the

presynaptic [Na^+] increased by 5.7 ± 1.1 mM (Fig. 1*B*), which is larger than the overall contribution of voltage-gated Na^+ channels and HCN channels at resting potential (Huang and Trussell, 2008, 2014). Increasing the spike frequency increased the Na^+ transients proportionately. Spikes at 10 Hz for 60 s increased the [Na^+] by 12.2 ± 1.7 mM, while 30 s of spikes at 20 Hz increased the [Na^+] by 16.3 ± 2.0 mM (Fig. 1). Since the total spike number was the same in these two experiments, the difference in [Na^+] increase likely reflects Na^+ extrusion, presumably by Na^+/K^+-ATPase activity. The calyx does not fire spontaneously in brain slices; however, it fires *in vivo* at frequencies >70 Hz in the absence of sound and up to 350 Hz with 80 dB tones (Lorteije et al., 2009). The presynaptic [Na^+] thus would be substantially higher *in vivo* than that in slice preparations, suggesting a mechanism that strongly modulates vesicle endocytosis *in vivo*. The presynaptic cytosolic [Na^+] is well correlated with the firing frequency and duration (Fig. 1), therefore precisely reflects the level of vesicle exocytosis.

We showed here that intracellular Na^+ accelerated slow and rapid endocytosis, and facilitated endocytosis overshoot. It is crucial to understand the molecular mechanism of how Na^+ modulates endocytosis. Previous studies demonstrated that cytosolic neurotransmitter concentration regulates vesicle cycling at GABAergic terminals in hippocampal cultures (Wang et al., 2013), and the neurotransmitter concentration rapidly controls vesicular neurotransmitter contents (Hori and Takahashi, 2012; Apostolides and Trussell, 2013). Na^+/H^+ exchangers are expressed on synaptic vesicles (Goh et al., 2011). The elevated cytosolic Na^+ activates vesicular Na^+/H^+ exchangers and regulates vesicular glutamate uptake (Huang and Trussell, 2014; Li et al., 2020), suggesting that Na^+ may modulate the endocytosis rate via changing vesicular contents. We tested this hypothesis. However, our results showed that neither slow nor rapid modes of endocytosis were influenced by the cytosolic glutamate concentration (Fig. 5). These results are consistent with previous experiments in the calyx of Held (Hori and Takahashi, 2012; Takami et al., 2017). Isotypes of Na^+/H^+ exchanger, which transports Na^+ into and H^+ out of the cell, are also expressed on plasma membrane. By interacting plasma membrane Na^+/H^+ exchangers, Na^+ may control intracellular pH, which in turn affects clathrin assembly and endocytosis (Morgan et al., 2003). In our electrophysiology and imaging recordings, the intracellular solutions contained 10 mM HEPES and were buffered to pH 7.3, which would minimize the pH change during endocytosis recordings. Moreover, by affecting the Na^+/H^+ exchanger, higher intracellular Na^+ would lower intracellular pH (intracellular acidification). However, a previous study showed that a rise in intracellular alkalization facilitates endocytosis (Zhang et al., 2010), which would be opposite to the proposal if Na^+ modulates endocytosis by controlling the activity of plasma membrane Na^+/H^+ exchangers. Na^+-activated K^+ channels are also expressed in the calyx terminal (Kaczmarek et al., 2005); however, the endocytosis was measured under Cs^+-based intracellular solutions, which would preclude the possible contribution of K^+ channels.

Another possible mechanism underlying the effects of Na^+ on endocytosis is the modulation of intracellular Ca^{2+}. Na^+ has been shown to affect presynaptic Ca^{2+} homeostasis through controlling the Na^+/Ca^{2+} exchanger activity (Kim et al., 2005), while Ca^{2+} plays specific roles in synaptic vesicle endocytosis (Leitz and Kavalali, 2016). Our results showed that changes in extracellular Na^+ or inhibition of NCX activity did not affect the endocytosis rate (Fig. 6), and that cytosolic Na^+ did not affect spike-evoked Ca^{2+} transients or decay, hence implying that the role of Na^+ in accelerating endocytosis is unlikely to be mediated by controlling intracellular Ca^{2+} level and Ca^{2+}-dependent pathways. Moreover, a previous study showed that subpicoampere Ca^{2+} influx has a profound effect on exocytosis (Awatramani et al., 2005), while we recently showed that Na^+ does not affect exocytosis or neurotransmitter release probability (Li et al., 2020), indicating that changes in intracellular [Na^+] have hardly any effect on basal Ca^{2+} level. The Ca^{2+} imaging may not be able to distinguish the Ca^{2+} change at nanodomains; however, previous studies showed that bulk Ca^{2+} would be primarily involved in endocytosis during repetitive simulations at the calyx of Held at similar ages (Yamashita et al., 2010).

The underlying mechanisms are not known. Recent studies showed that Na^+ is involved in the activation of endocytic protein dynamin (Chappie et al., 2010) as it allosterically modulates different G-proteins (Vickery et al., 2018), suggesting a possible interaction of Na^+ with endocytic machinery. However, the blocking of dynamin fully disrupts the endocytosis (Hosoi et al., 2009). New approaches are needed to better separate these processes experimentally.

We showed here that presynaptic cytosolic Na^+ accelerated both slow and rapid forms of endocytosis and facilitated endocytosis overshoot. During high-frequency synaptic transmission, large numbers of synaptic vesicles are fused and Na^+ concomitantly accumulated in the presynaptic cytosol. Na^+ facilitates vesicle endocytosis (Figs. 1–3) and vesicular glutamate uptake (Li et al., 2020). Hence, Na^+ works as a signal to coordinate vesicle endocytosis and vesicular glutamate uptake according to the level of exocytosis, representing a novel mechanism of vesicle exoendocytosis coupling that sustains neurotransmission at high frequency.

References

Alés E, Tabares L, Poyato JM, Valero V, Lindau M, Alvarez de Toledo G (1999) High calcium concentrations shift the mode of exocytosis to the kiss-and-run mechanism. Nat Cell Biol 1:40–44.

Apostolides PF, Trussell LO (2013) Rapid, activity-independent turnover of vesicular transmitter content at a mixed glycine/GABA synapse. J Neurosci 33:4768–4781.

Awatramani GB, Price GD, Trussell LO (2005) Modulation of transmitter release by presynaptic resting potential and background calcium levels. Neuron 48:109–121.

Balaji J, Armbruster M, Ryan TA (2008) Calcium control of endocytic capacity at a CNS synapse. J Neurosci 28:6742–6749.

Chappie JS, Acharya S, Leonard M, Schmid SL, Dyda F (2010) G domain dimerization controls dynamin's assembly-stimulated GTPase activity. Nature 465:435–440.

Elhamdani A, Azizi F, Artalejo CR (2006) Double patch clamp reveals that transient fusion (kiss-and-run) is a major mechanism of secretion in calf adrenal chromaffin cells: high calcium shifts the mechanism from kiss-and-run to complete fusion. J Neurosci 26:3030–3036.

Fedchyshyn MJ, Wang LY (2005) Developmental transformation of the release modality at the calyx of Held synapse. J Neurosci 25:4131–4140.

Fernández-Alfonso T, Ryan TA (2004) The kinetics of synaptic vesicle pool depletion at CNS synaptic terminals. Neuron 41:943–953.

Goh GY, Huang H, Ullman J, Borre L, Hnasko TS, Trussell LO, Edwards RH (2011) Presynaptic regulation of quantal size: K^+/H^+ exchange stimulates vesicular glutamate transport. Nat Neurosci 14:1285–1292.

Granseth B, Odermatt B, Royle SJ, Lagnado L (2006) Clathrin-mediated endocytosis is the dominant mechanism of vesicle retrieval at hippocampal synapses. Neuron 51:773–786.

Holt M, Cooke A, Wu MM, Lagnado L (2003) Bulk membrane retrieval in the synaptic terminal of retinal bipolar cells. J Neurosci 23:1329–1339.

Hori T, Takahashi T (2012) Kinetics of synaptic vesicle refilling with neurotransmitter glutamate. Neuron 76:511–517.

Hosoi N, Holt M, Sakaba T (2009) Calcium dependence of exo- and endocytotic coupling at a glutamatergic synapse. Neuron 63:216–229.
Huang H, Trussell LO (2008) Control of presynaptic function by a persistent Na(+) current. Neuron 60:975–979.
Huang H, Trussell LO (2014) Presynaptic HCN channels regulate vesicular glutamate transport. Neuron 84:340–346.
Kaczmarek LK, Bhattacharjee A, Desai R, Gan L, Song P, von Hehn CA, Whim MD, Yang B (2005) Regulation of the timing of MNTB neurons by short-term and long-term modulation of potassium channels. Hear Res 206:133–145.
Kim MH, Korogod N, Schneggenburger R, Ho WK, Lee SH (2005) Interplay between Na^+/Ca^{2+} exchangers and mitochondria in Ca^{2+} clearance at the calyx of Held. J Neurosci 25:6057–6065.
Koch M, Holt M (2012) Coupling exo- and endocytosis: an essential role for PIP(2) at the synapse. Biochim Biophys Acta 1821:1114–1132.
Kononenko NL, Haucke V (2015) Molecular mechanisms of presynaptic membrane retrieval and synaptic vesicle reformation. Neuron 85:484–496.
Leitz J, Kavalali ET (2016) Ca2+ Dependence of Synaptic Vesicle Endocytosis. Neuroscientist 22:464–476.
Li D, Zhu Y, Huang H (2020) Spike activity regulates vesicle filling at a glutamatergic synapse. J Neurosci 40:4972–4980.
Lindau M, Neher E (1988) Patch-clamp techniques for time-resolved capacitance measurements in single cells. Pflugers Arch 411:137–146.
Lorteije JA, Rusu SI, Kushmerick C, Borst JG (2009) Reliability and precision of the mouse calyx of Held synapse. J Neurosci 29:13770–13784.
Morgan JR, Prasad K, Jin S, Augustine GJ, Lafer EM (2003) Eps15 homology domain-NPF motif interactions regulate clathrin coat assembly during synaptic vesicle recycling. J Biol Chem 278:33583–33592.
Orlando M, Schmitz D, Rosenmund C, Herman MA (2019) Calcium-independent exo-endocytosis coupling at small central synapses. Cell Rep 29:3767–3774.e3.
Regehr WG (2012) Short-term presynaptic plasticity. Cold Spring Harb Perspect Biol 4:a005702.
Renden R, von Gersdorff H (2007) Synaptic vesicle endocytosis at a CNS nerve terminal: faster kinetics at physiological temperatures and increased endocytotic capacity during maturation. J Neurophysiol 98: 3349–3359.
Rose CR (2012) Two-photon sodium imaging in dendritic spines. Cold Spring Harb Protoc 2012:1161–1165.
Sankaranarayanan S, Ryan TA (2001) Calcium accelerates endocytosis of vSNAREs at hippocampal synapses. Nat Neurosci 4:129–136.
Soykan T, Kaempf N, Sakaba T, Vollweiter D, Goerdeler F, Puchkov D, Kononenko NL, Haucke V (2017) Synaptic vesicle endocytosis occurs on multiple timescales and is mediated by formin-dependent actin assembly. Neuron 93:854–866.e4.
Spratt PWE, Ben-Shalom R, Keeshen CM, Burke KJ Jr, Clarkson RL, Sanders SJ, Bender KJ (2019) The autism-associated gene Scn2a contributes to dendritic excitability and synaptic function in the prefrontal cortex. Neuron 103:673–685.e5.
Sudhof TC (2004) The synaptic vesicle cycle. Annu Rev Neurosci 27:509–547.
Sun JY, Wu LG (2001) Fast kinetics of exocytosis revealed by simultaneous measurements of presynaptic capacitance and postsynaptic currents at a central synapse. Neuron 30:171–182.
Sun JY, Wu XS, Wu LG (2002) Single and multiple vesicle fusion induce different rates of endocytosis at a central synapse. Nature 417:555–559.
Sun T, Wu XS, Xu J, McNeil BD, Pang ZP, Yang W, Bai L, Qadri S, Molkentin JD, Yue DT, Wu LG (2010) The role of calcium/calmodulin-activated calcineurin in rapid and slow endocytosis at central synapses. J Neurosci 30:11838–11847.
Takami C, Eguchi K, Hori T, Takahashi T (2017) Impact of vesicular glutamate leakage on synaptic transmission at the calyx of Held. J Physiol 595:1263–1271.
Vickery ON, Carvalheda CA, Zaidi SA, Pisliakov AV, Katritch V, Zachariae U (2018) Intracellular transfer of Na(+) in an active-state g-protein-coupled receptor. Structure 26:171–180.e2.
von Gersdorff H, Borst JG (2002) Short-term plasticity at the calyx of Held. Nat Rev Neurosci 3:53–64.
von Gersdorff H, Matthews G (1994) Inhibition of endocytosis by elevated internal calcium in a synaptic terminal. Nature 370:652–655.
Wang L, Tu P, Bonet L, Aubrey KR, Supplisson S (2013) Cytosolic transmitter concentration regulates vesicle cycling at hippocampal GABAergic terminals. Neuron 80:143–158.
Wu LG, Betz WJ (1996) Nerve activity but not intracellular calcium determines the time course of endocytosis at the frog neuromuscular junction. Neuron 17:769–779.
Wu LG, Borst JG (1999) The reduced release probability of releasable vesicles during recovery from short-term synaptic depression. Neuron 23:821–832.
Wu LG, Hamid E, Shin W, Chiang HC (2014) Exocytosis and endocytosis: modes, functions, and coupling mechanisms. Annu Rev Physiol 76:301–331.
Wu W, Wu LG (2007) Rapid bulk endocytosis and its kinetics of fission pore closure at a central synapse. Proc Natl Acad Sci U S A 104:10234–10239.
Wu W, Xu J, Wu XS, Wu LG (2005) Activity-dependent acceleration of endocytosis at a central synapse. J Neurosci 25:11676–11683.
Wu XS, Wu LG (2014) The yin and yang of calcium effects on synaptic vesicle endocytosis. J Neurosci 34:2652–2659.
Wu XS, McNeil BD, Xu J, Fan J, Xue L, Melicoff E, Adachi R, Bai L, Wu LG (2009) Ca(2+) and calmodulin initiate all forms of endocytosis during depolarization at a nerve terminal. Nat Neurosci 12:1003–1010.
Xue L, McNeil BD, Wu XS, Luo F, He L, Wu LG (2012) A membrane pool retrieved via endocytosis overshoot at nerve terminals: a study of its retrieval mechanism and role. J Neurosci 32:3398–3404.
Yamashita T, Eguchi K, Saitoh N, von Gersdorff H, Takahashi T (2010) Developmental shift to a mechanism of synaptic vesicle endocytosis requiring nanodomain Ca2+. Nat Neurosci 13:838–844.
Yuan T, Liu L, Zhang Y, Wei L, Zhao S, Zheng X, Huang X, Boulanger J, Gueudry C, Lu J, Xie L, Du W, Zong W, Yang L, Salamero J, Liu Y, Chen L (2015) Diacylglycerol guides the hopping of clathrin-coated pits along microtubules for exo-endocytosis coupling. Dev Cell 35:120–130.
Zhang Y, Huang H (2017) SK channels regulate resting properties and signaling reliability of a developing fast-spiking neuron. J Neurosci 37:10738–10747.
Zhang Z, Nguyen KT, Barrett EF, David G (2010) Vesicular ATPase inserted into the plasma membrane of motor terminals by exocytosis alkalinizes cytosolic pH and facilitates endocytosis. Neuron 68:1097–1108.